Electronic Supplementary Material

The cooperation effect of Ni and Pt in the hydrogenation of acetic acid

Deng Pan[1,*], Jiahua Zhou[1,*], Bo Peng (✉)[2], Shengping Wang[1], Yujun Zhao (✉)[1], Xinbin Ma[1]

1 Key Laboratory for Green Chemical Technology of Ministry of Education, School of Chemical Engineering and Technology, Collaborative Innovation Center of Chemical Science and Engineering, Tianjin University, Tianjin 300072, China

2 SINOPEC Research Institute of Petroleum Processing (RIPP), Beijing 100083, China

E-mails: yujunzhao@tju.edu.cn (Zhao Y); pengbo.ripp@sinopec.com (Peng B)

1. Experimental

1.1 Chemicals

Tin (II) chloride ($SnCl_2$, > 98%), iron (III) chloride ($FeCl_3$, AR) and manganese nitrate ($Mg(NO_3)_2$, > 99.0%) were purchased from Aladdin. Zinc nitrate ($Zn(NO_3)_2$, 99%) was purchased from Tianjin Guangfu Fine Chemical Co., Ltd. Ethanol, copper (II) nitrate hydrate ($Cu(NO_3)_2 \cdot 3H_2O$, 99%) and ferrous chloride ($FeCl_2 \cdot 4H_2O$, 98.0%) were purchased from YuanLi Chemical Reagent Co., Ltd. The platinum (II) tetra-ammine chloride ($[Pt(NH_3)_4]Cl_2$, Pt > 55.4%) was purchased from Beijing HWRK Chemical Co., Ltd. Tetraethoxyorthosilicate (TEOS > 99.5%), ammonium hydroxide (NH_3 25% ~ 28%), ferric nitrate ($Fe(NO_3)_3 \cdot 9H_2O$, 99%), nickel chloride ($NiCl_2 \cdot 6H_2O$, 98.0%), nickel nitrate ($Ni(NO_3)_2 \cdot 6H_2O$, 98.0%), cobalt nitrate

($Co(NO_3)_2 \cdot 6H_2O$, 99.0%), cerium (III) nitrate hexahydrate ($Ce(NO_3)_3 \cdot 6H_2O$, 99.5%) and cobalt chloride ($CoCl_2 \cdot 6H_2O$, 99.0%) were purchased from Tianjin Kermel Chemical Co., Ltd.

1.2 Catalyst Characterization

Fourier transform infrared (FTIR) analysis was performed on calcined catalyst on a Thermo Scientific Nicolet 6700 (32 scans, $4cm^{-1}$). For the catalyst, it is compressed and placed in the in-situ cell. The FTIR spectra was recorded from 400-$4000cm^{-1}$ with a resolution of 4 cm^{-1}.

1.3 Catalytic performance

The gas-phase catalytic hydrogenation of acetic acid was carried out in a stainless-steel tubular fixed-bed reactor with an inner diameter of 8 mm. In a typical operation, 0.65 g (40-60 mesh) catalyst was placed at the center of the reactor, and both sides of the catalyst bed were packed with quartz powder (20-40 mesh). Prior to the reaction, the catalyst was reduced in H_2 flow (99.999%, 100 mL $\cdot min^{-1}$) at 300 ℃ for 4 hours. Then AcOH (99.5%) was fed into the reactor using a constant-flow pump and vaporized through a preheater maintained at 200 ℃. Catalytic test was performed under 2.6 MPa at 270 ℃, with a weight hourly space velocity (WHSV) of AcOH of 1 ~ 3 h^{-1}. The collected products in the condenser were analyzed on a gas chromatogragh (BEIFEN 3420A) equipped with an HP-INNOWAX capillary column (30 m × 0.25 mm × 0.25 μm) and a flame ionization detector (FID). Multiple samples were taken under the same experimental conditions and the results were averaged to

ensure the reproducibility.

2. Catalyst Characterization

2.1 XRD

The XRD results of reduced catalysts are shown in Fig. 3. The broad diffraction peak at 2θ = 22 ° is attributed to the amorphous SiO_2 support. The characteristic diffraction peak of Pt, Sn and Ni cannot be observed on these catalysts because of the much lower loading and higher dispersion. The size of metal nanoparticles is under the detection limitation of XRD method.

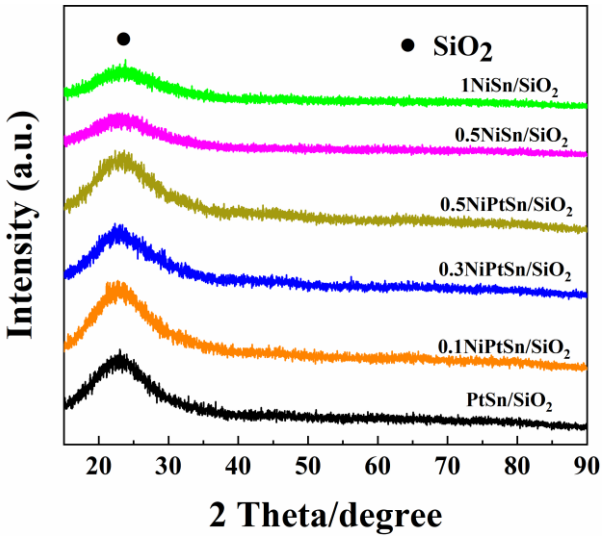

Fig. S1 XRD patterns of reduced catalysts

2.2 XPS

The chemical states and the surface composition of the catalysts were studied by XPS. Considering only trace amount of Ni existed in 0.1Ni-PtSn-IW catalyst, the change in the surface electron density of Pt nanoparticles induced by the Ni dopant cannot be

accurately detected with reliability. Therefore, the 0.3Ni-PtSn-IW catalyst was chosen as the probe catalyst for the comparison with NiSn-IW and PtSn catalysts.

The Ni 2p spectra peaks refer to the Ni^0 and Ni^{2+} species while the Pt 4f spectra peaks are ascribed to Pt^0 and Pt^{2+} species in Fig. 10. The Ni^0 2p 3/2 spectra peak of 0.3Ni-PtSn-IW catalyst shows a higher BE of 855.43 eV than that (854.55 eV) of 0.3NiSn-IW catalyst, indicating the decrease of electron density of Ni surface. Meanwhile, the Pt 4f 7/2 spectra peak located at 71.63 eV for PtSn catalyst shifts to 71.62 eV for the 0.3Ni-PtSn-IW catalyst. The negligible shift of Pt 4f 7/2 spectra peak can be attributed to the tiny amount of Ni, whose impact on the surface electron density of Pt species can be ignored since more Pt species having no interaction with Ni species are presented on the catalyst.

The strong interaction between Ni and Pt can increase the number of activated H atoms and improve the catalytic performance [1]. The above results further prove that the addition of Ni can form a strong interaction between Pt and Ni species, which benefits the dispersion of Pt species, resulting in a high catalytic activity. What's more, the interaction between Ni and Pt can lead to a hydrogen-rich environment due to the H atoms spillover from Pt to Ni species.

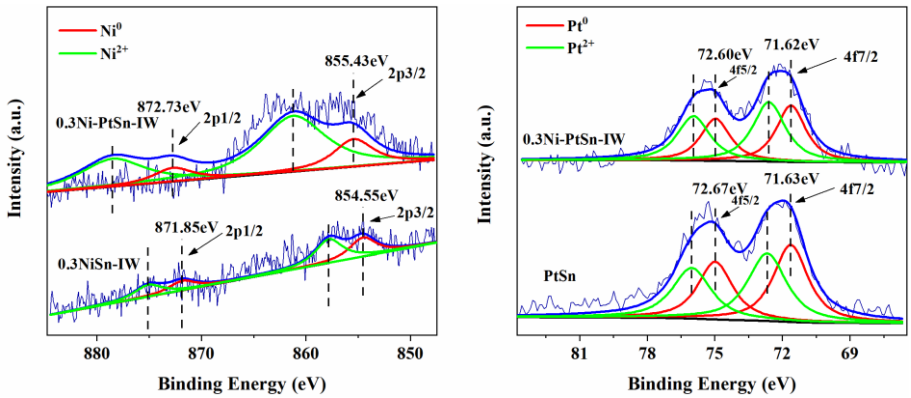

Fig. S2. XPS spectra of reduced catalysts

2.3 FT-IR

As shown in Fig. S3, the IR band at 3432 cm^{-1} is attributed to the hydroxyl groups on the catalyst surface while the bands at 800 cm^{-1} and 1100 cm^{-1} are attributed to the stretching vibration and anti-stretching vibration of Si-O-Si band, respectively. With the excessive introduction of Ni, there is a significant decrease on the above IR band from the recorded IR spectra, indicating the consumption of hydroxyl groups. Also, the anchoring of Pt precursor on the support by SEA method need hydroxyl groups on the surface support, but excessive Ni dopant can occupy more surface hydroxyl groups of silica, which has been evidenced by the FT-IR result.

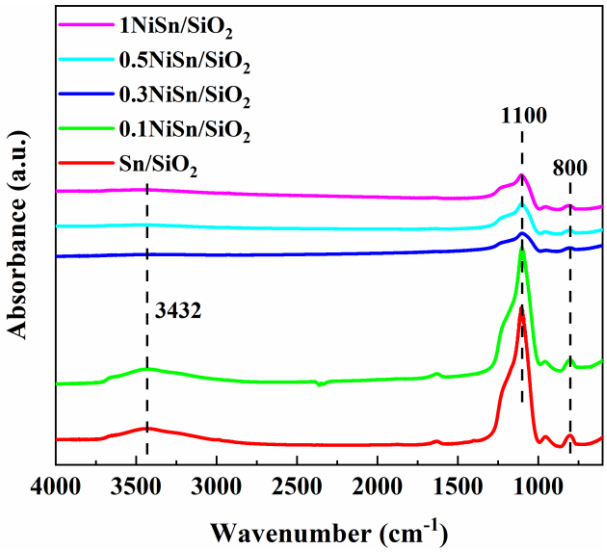

Fig. S3 FT-IR spectra of xNiSn/SiO_2 samples

2.4 TEM

As shown in Fig. S4, Ni, Pt and Sn are dispersed evenly on SiO_2 support. This result is in agreement with the above speculation of the interaction between Ni dopant and other surface species.

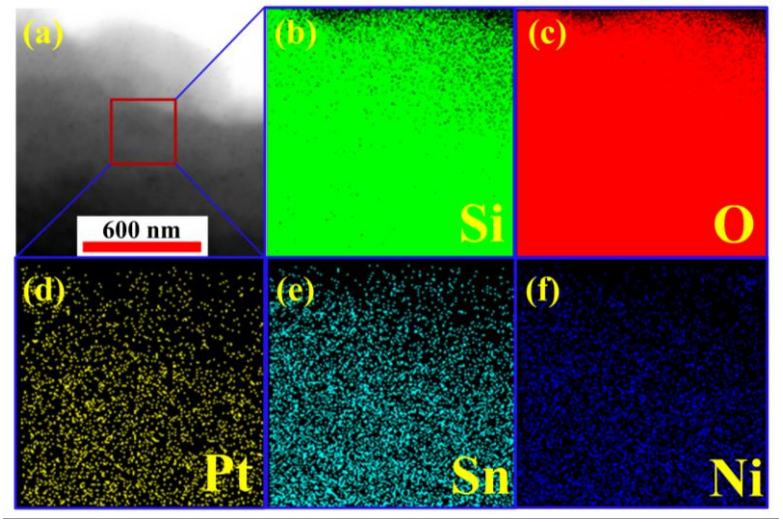

Fig. S4. STEM-EDS mapping of 0.1Ni-PtSn-IW catalyst after reduction, (a) 0.1Ni-PtSn-IW, (b) Si distribution, (c) O distribution, (d) Pt distribution, (e) Sn distribution, (f) Ni distribution

For the best catalyst, the Ni loading is only about 0.1 wt.%, therefore, it is difficult to find intermetallic compounds or alloys through their TEM images. In order to study the interaction between Pt and Ni, HRTEM of 0.3Ni-PtSn/IW catalyst was further performed. As shown in Fig. S5, some of the Ni species has an interaction with Pt species while other excessive Ni species were loaded on the support alone. This structure can be attributed to the catalyst preparation process, in which Ni and Pt precursors were loaded onto the support sequentially by the impregnation method. Meanwhile, there is no alloy formation according to the HRTEM results.

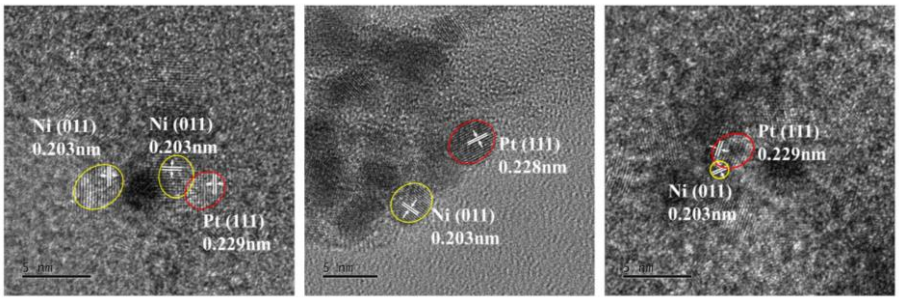

Fig. S5. HRTEM images of 0.3Ni-PtSn/IW catalyst

3. Effect of Ni dopant on the catalytic performance

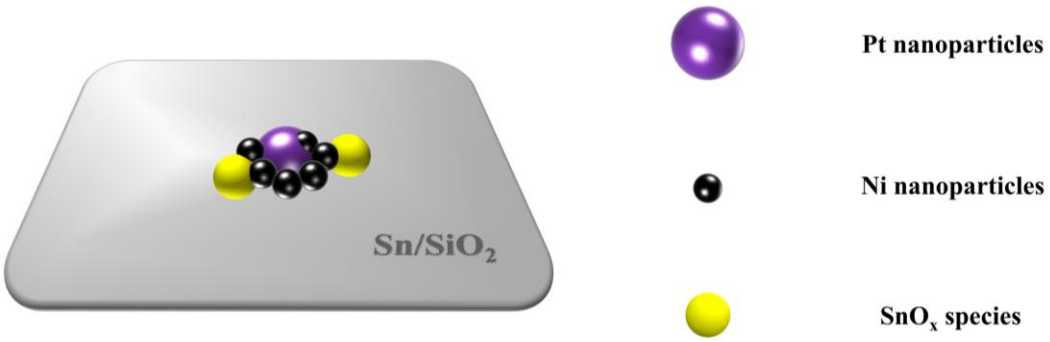

Fig. S6. Schematic diagram of excessive Ni dopant

Reference

1. Li Y, Lai G-H, Zhou R-X. Carbon nanotubes supported Pt-Ni catalysts and their properties for the liquid phase hydrogenation of cinnamaldehyde to hydrocinnamaldehyde. Applied Surface Science, 2007, 253(11): 4978-4984.